The Canadian Mineralogist
Vol. 36, pp. 147-162 (1998)

LOW-TEMPERATURE FAYALITE, GREENALITE, AND MINNESOTAITE FROM THE OVERLOOK GOLD DEPOSIT, WASHINGTON: PHASE RELATIONS IN THE SYSTEM $FeO–SiO_2–H_2O$

MICHAEL G. RASMUSSEN

Echo Bay Minerals Co., 921 Fish Hatchery Road, Republic, Washington 99166, U.S.A.

BERNARD W. EVANS[1] AND SCOTT M. KUEHNER

Department of Geological Sciences, Box 351310, University of Washington, Seattle, Washington 98195-1310, U.S.A.

ABSTRACT

At the Overlook gold mine in northeastern Washington, a fayalite-bearing assemblage of iron silicates, magnetite, and pyrrhotite, plus quartz and calcite, formed during alteration of a Permian volcanogenic, carbonate-rich, massive magnetite–sulfide seafloor deposit. The temperature of fluid inclusion homogenization, oxygen isotope ratios, and phase equilibrium calculations constrain the temperature of the fayalite-forming environment to approximately 300°C. The fayalite is close to end-member composition, $Fa_{95–98}$, and the greenalite and minnesotaite are correspondingly Fe-rich. No grunerite has been found. The paragenetic sequence fayalite → greenalite → minnesotaite → quartz represents infiltration at approximately 300°C of an initially very reducing, Fe-rich hydrothermal fluid that became progressively more SiO_2-rich. Provisional thermodynamic data for greenalite are presented, and these are used to construct P–T–$a(SiO_2)$ phase diagrams for the system $FeO–SiO_2–H_2O$. Phase relations in this system differ topologically from those in the analogue system $MgO–SiO_2–H_2O$ by virtue of the H_2O-conserved reaction: talc + olivine = MgFe-amphibole + serpentine, which proceeds from left to right with an increase in Fe:Mg ratio of the system. One sample contains in addition to greenalite an iron-dominant serpentine with ideal serpentine stoichiometry, Fe : Si = 3 : 2.

Keywords: hydrothermal fayalite, greenalite, minnesotaite, FMSH system, Overlook gold mine, Washington.

SOMMAIRE

À la mine d'or de Overlook, dans le secteur nord-est de l'état de Washington, nous avons découvert un assemblage à fayalite contenant des silicates de fer, magnétite et pyrrhotite, en plus de quartz et calcite, formé lors de l'altération au permien d'un amas de magnétite et de sulfures d'origine volcanogénique, riche en carbonate, issu d'un milieu de ride océanique. La température d'homogénéisation des inclusions fluides, les rapports isotopiques de l'oxygène, et les calculs des relations de phases à l'équilibre limitent la température du milieu de formation de la fayalite à environ 300°C. La fayalite possède une composition proche du pôle, $Fa_{95–98}$, et la greenalite de même que la minnesotaïte lui sont conformes dans leurs teneurs en fer. Nous n'avons pas signalé de grunerite. La séquence paragénétique fayalite → greenalite → minnesotaïte → quartz résulterait d'une infiltration à environ 300°C d'une phase fluide hydrothermale très réductrice et riche en fer au début, qui est par la suite devenue progressivement plus siliceuse. Nous présentons des données thermodynamiques provisoires pour la greenalite, et nous nous en servons pour construire des diagrammes pour le système $FeO–SiO_2–H_2O$ ayant comme axes P–T–$a(SiO_2)$. Les relations de phases dans ce système se distinguent par leur topologie de celles dans le système analogue $MgO–SiO_2–H_2O$ à cause de la conservation de H_2O au cours de la réaction talc + olivine = amphibole à Mg,Fe + serpentine, qui procède vers la droite avec une augmentation du rapport Fe:Mg dans le système. Un échantillon contient, en plus de la greenalite, une serpentine à dominance de fer dont la stoechiométrie est celle d'une serpentine classique (Fe : Si = 3 : 2).

(Traduit par la Rédaction)

Mots-clés: fayalite hydrothermale, greenalite, minnesotaïte, système FMSH, mine d'or de Overlook, Washington.

INTRODUCTION

Fayalite is well known in plutonic and volcanic igneous rocks of high Fe:Mg ratio, such as ferrogabbro, ferrodiorite, syenite, granite, granite pegmatite, granophyre, dacite and rhyolite. In metamorphic rocks, fayalite is a product of high-grade contact and regional metamorphism of banded iron-formation and high-(Fe/Mg) igneous protoliths, where pressures were lower than those required to replace fayalite with

[1] *E-mail address:* bwevans@u.washington.edu

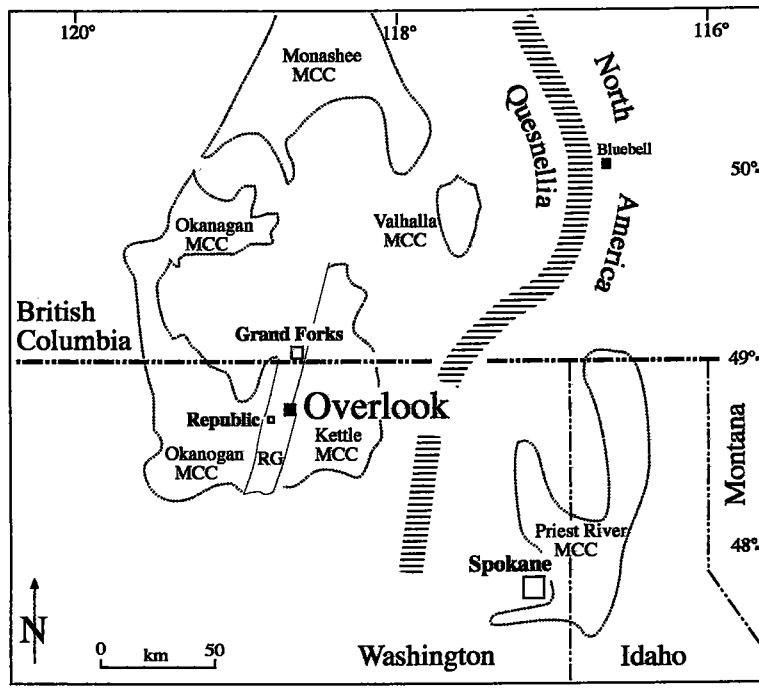

FIG. 1. Index map of major structural and tectonic features of the southern terminus of the Omineca Crystalline Belt. RG: Republic Graben, MCC: metamorphic core complex.

ferrosilite. At low to medium metamorphic grades, fayalite is ordinarily excluded from iron-rich metasediments for two reasons: the presence of quartz and of an aqueous or carbonic pore fluid. Their presence results instead in the formation of Fe-silicate hydrates such as grunerite, minnesotaite, and greenalite, and carbonates such as siderite and ankerite. As a result, few occurrences of low- or medium-temperature fayalite in metamorphic or hydrothermal environments have been described. In those that have, quartz is absent (or was at one time), and the olivine is typically manganoan, in many cases tephroite or in the compositional range that has been called "knebelite" (*e.g.*, Russell 1946, Alpers 1980, Birch 1984). The Bluebell Zn–Pb–Ag mine in southeastern British Columbia (Fig. 1) contains among the gangue minerals a manganoan iron-rich olivine, $Fa_{58-69}Tep_{28-38}$ (Gunning 1936, Shannon 1970, Mossman & Pawson 1976), inferred to have formed by replacement of limestone below 450°C (Ohmoto & Rye 1970). Manganoan fayalite formed early, followed by sulfide – quartz – carbonate ore, together with manganoan minnesotaite and greenalite. At the Overlook gold deposit in northeastern Washington (Fig. 1), we have found nearly end-member fayalite in similar parageneses, and estimate temperatures of formation in the range 280 to 320°C. We believe this to be the lowest well-documented temperature for the crystallization of nearly end-member fayalite in nature. The occurrence provides clues to the stability relations of fayalite and helps confirm calculated phase-equilibria at low temperatures for minerals in the system $FeO–SiO_2–H_2O$. Because its thermodynamic properties are well known (*e.g.*, Robie *et al.* 1978, 1982, Thierry *et al.* 1981, Berman 1988, Holland & Powell 1990), fayalite serves as a convenient thermodynamic reference-phase for the less well characterized Fe-silicate hydrates, a role that is enhanced by its stability over a very large range in temperature.

At Overlook, the principal ore minerals (*i.e.*, gold-hosting) are magnetite, pyrrhotite, and chalcopyrite, which formed in a Permian back-arc sea-floor environment from exhaled hydrothermal fluid. The iron silicate assemblage described in this paper postdates formation of the iron oxides and sulfides, and is indirectly constrained by deposit-scale mesoscopic and microscopic features to have formed during Eocene magmatism and hydrothermal activity (Rasmussen 1993). Gold is distributed throughout the Overlook deposit, without positive or negative correlation to the iron silicate assemblages, which occur primarily in massive magnetite zones (Fig. 2).

In this paper, we describe the geological setting of the Overlook mine and the Fe-rich silicates of

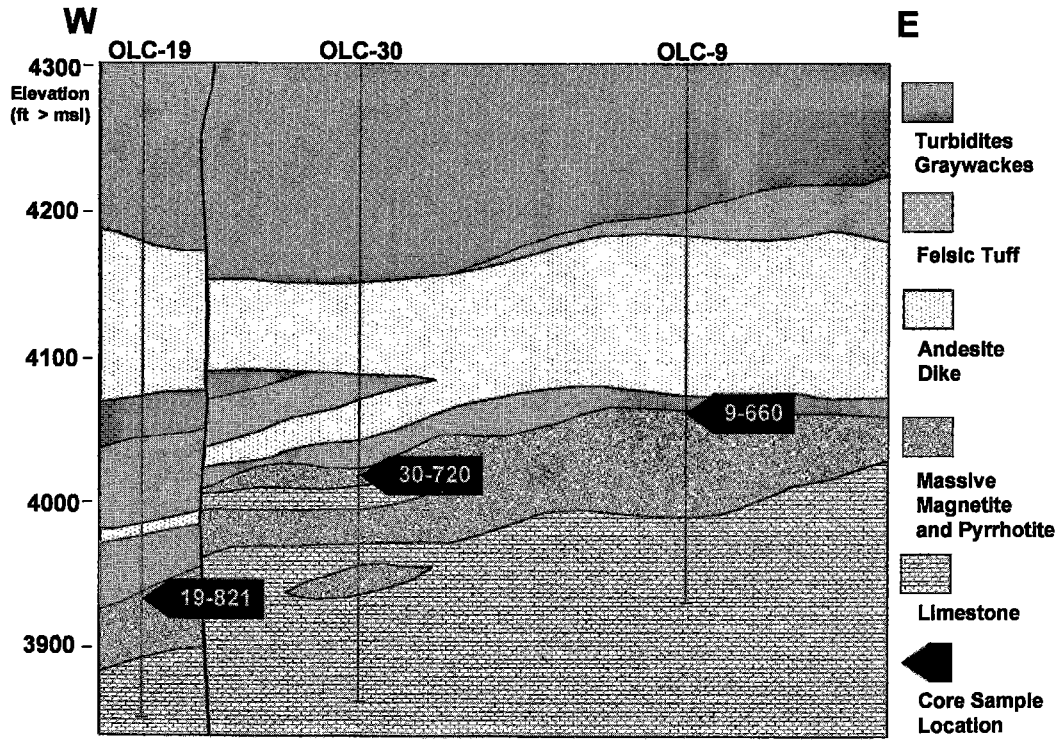

FIG. 2. Simplified E–W vertical cross-section through the northern portion of the Overlook gold deposit, showing drill-core and sample locations. No vertical exaggeration.

hydrothermal origin within it. The mineral assemblages, textures, sequences of parageneses, mineral compositions, and temperature estimates provide support for an origin at approximately 300°C in initially quartz-undersaturated, carbonate-bearing rocks, infiltrated by a highly reduced, compositionally evolving hydrothermal fluid.

GEOLOGICAL SETTING

The Overlook gold deposit is one of four gold-enriched volcanogenic massive magnetite–sulfide deposits on a stratigraphic horizon within lower-greenschist-facies metasedimentary rocks of the Permian Attwood Formation (Rasmussen 1993, 1995). The Overlook deposit was mined in 1990–1992. The Key East deposit (Lowe & Larson 1996) and the Key West deposit were mined out in 1993. The Lamefoot deposit has been mined since 1994.

The Attwood Formation (Church 1986, Fyles 1990, 1995) contains arc-derived clastic and carbonate rocks of the Harper Ranch sub-terrane of Quesnellia (Wheeler *et al.* 1991, Monger *et al.* 1991, Nelson *et al.* 1995), a terrane of oceanic and island-arc rocks accreted to North America in early- to mid-Jurassic time (Monger *et al.* 1982). Quesnellian rocks that host the Overlook deposit are preserved in the Republic Graben (Fig. 1), a north-trending Tertiary structure 15 km across and 110 km long that separates two metamorphic core complexes of the southern Omineca Belt (Orr & Cheney 1987, Parrish *et al.* 1988). In the vicinity of the Republic Graben, the Attwood Formation structurally underlies ophiolitic rocks of the Knob Hill Group (Church 1986, Fyles 1990, 1995, Cheney & Rasmussen 1996). Regionally, the Attwood Formation is interpreted to have formed in a back-arc setting adjacent to a rising volcanic complex above a late Paleozoic subduction zone (Roback & Walker 1995). At the Overlook site, Attwood rocks are overturned by fold-and-thrust deformation related to Jurassic accretion and vertical rotation in the upper plate of the Eocene Kettle Metamorphic Complex (Rasmussen 1993, Wingate & Irving 1994, Cheney & Rasmussen 1996).

Geology of Overlook Orebody

The structural footwall of the overturned Overlook deposit (Fig. 2) consists of limestone overlain by auriferous massive to semimassive magnetite and pyrrhotite in a north–northwest-trending oblate body 200 × 75 meters in plan and 2–15 meters thick. Massive ores are overlain by the stratigraphic footwall of the deposit: fine-grained sulfidic, tuffaceous sediments 5–15 meters thick, with chert-pebble conglomerates in seams and lenses. The tuffaceous rocks are (structurally) overlain by a 100–200-meter section of pelitic turbidites, greywackes and chert-pebble conglomerates. Quartz–sulfide veinlets in rocks above stratiform massive ore also host economic concentrations of gold. Similar veins at the Lamefoot mine represent Jurassic ($^{40}Ar/^{39}Ar_{sericite}$ = 197 ± 3 Ma: Archibald 1996) mesothermal veining and sericitization of the original footwall (Rasmussen 1993, 1995).

The volcanogenic portion of the Overlook orebody consists of massive magnetite, massive pyrrhotite, and gradations between the two, with variable amounts of gangue calcite, quartz and talc; these are locally accompanied by greenalite, minnesotaite, fayalite (or "iddingsite") and ilvaite. Massive magnetite ranges from cryptically bedded, homogeneous early magnetite to brecciated magnetite intergrown with iron silicate minerals, calcite, and quartz. Late replacive magnetite is pseudomorphic after fayalite and also occurs as cross-cutting veins within silicate-rich early magnetite. Layering in the unbrecciated, homogeneous magnetite is defined primarily by subtle differences in modal amount and grain size of magnetite. Magnetite-bearing rocks constitute 75% of the massive portion of the orebody. The assemblage of iron silicate minerals fayalite, greenalite, and minnesotaite occurs paragenetically between brecciated early magnetite and late replacive magnetite.

Massive pyrrhotite accounts for about 20% of the massive ore, and occurs as tabular to irregular, lensoid bodies one to three meters thick and tens of meters long at the stratigraphic base of the massive zone. The lenses are >70% pyrrhotite and exhibit thin layering defined by interbeds of quartz and ferroan talc; folds in the pyrrhotite are either tectonic or soft-sediment features.

The Overlook deposit is intruded by two sets of post-mineralization dikes. The younger set consists of biotite trachyandesite, the biotite of which has been dated at 52.0 ± 0.5 Ma (Archibald 1996: Lamefoot deposit, $^{40}Ar/^{39}Ar$ laser total fusion and step-heating). The older dikes consist of sericite–carbonate-altered hornblende diorite of undetermined age. We interpret the iron silicate minerals described in this paper to have formed during hydrothermal alteration of an oxide-rich Permian volcanogenic massive sulfide deposit. The hydrothermal process consisted of a broadly isothermal series of reactions in which carbonate minerals were replaced by fayalite and greenalite in rock consisting of carbonate, sulfide, and (early) magnetite. Increasing hydrothermal enrichment of silica resulted in formation of greenalite + minnesotaite followed by minnesotaite + quartz assemblages. Late quartz formed fracture-filling veinlets and irregular embayments of the iron silicate minerals.

Lowe & Larson (1996) argued that the massive magnetite–sulfide deposits of the district are skarns related to the intrusion of the biotite trachyandesite dikes. Their interpretation is based on: (1) the occurrence of andradite and clinopyroxene in the massive ores of the Key East deposit (located 2 km northeast of Overlook) and (2) the trend of decreasing $\delta^{18}O$ values in dike samples with decreasing distance from zones of mineralization. However, the skarn model fails to account for several lines of evidence indicating a seafloor origin for the massive ores. These were described in Rasmussen (1993) and include the following: (1) sedimentary layering in the massive ores, (2) base-metal zonation from a Cu-rich base to Zn-rich top, (3) chlorite – sericite – pyrite – chalcopyrite alteration of felsic volcaniclastic footwall rocks, and (4) a thick (6–9 m) conglomerate overlying the orebody containing abundant clasts of gold-rich pyrrhotite and magnetite. The calc-silicate minerals observed by Lowe & Larson (1996) are possible analogues of the Fe-silicate assemblage at Overlook (which includes ilvaite). In this case, the oxygen isotopic data at Key East provide a possible link between the iron silicate minerals at Overlook and the 52.0 ± 0.5 Ma biotite trachyandesite intrusions. However, we cannot rule out the possibility, especially in light of recent work on the Bald Mountain massive sulfide deposit, Maine (Slack *et al.* 1997, Foley *et al.* 1997), that the Overlook iron silicates formed during late-stage hydrothermal alteration within the Permian oxide – sulfide – carbonate seafloor mound.

Iron Silicate Minerals

Fresh fayalite was identified in three drill cores in the NW portion of the orebody (Fig. 2). The samples occur in calcite-bearing magnetite-rich rock immediately below a contact with felsic volcaniclastic rock. Distinctive pseudomorphs of "iddingsite", magnetite, pyrrhotite, and ilvaite indicate that fayalite was formerly more widespread in the magnetite-rich horizon. In hand sample, small dark reddish brown circular to elongate spots 1 to 10 mm in long dimension occur in a heterogeneous green to brown rock composed of magnetite, pyrrhotite, greenalite, minnesotaite, calcite, ilvaite and quartz. The reddish brown spots are concentrations of "iddingsite" that in thin section are seen to have partially to completely replaced clusters of semiradiating blades of idiomorphic fayalite (Figs. 3a, b, c) up to 1 mm in length. The texture of the fayalite is identical to that of the manganoan fayalite at the Bluebell mine (Mossman & Pawson 1976, Figs. 3, 4). The fayalite is

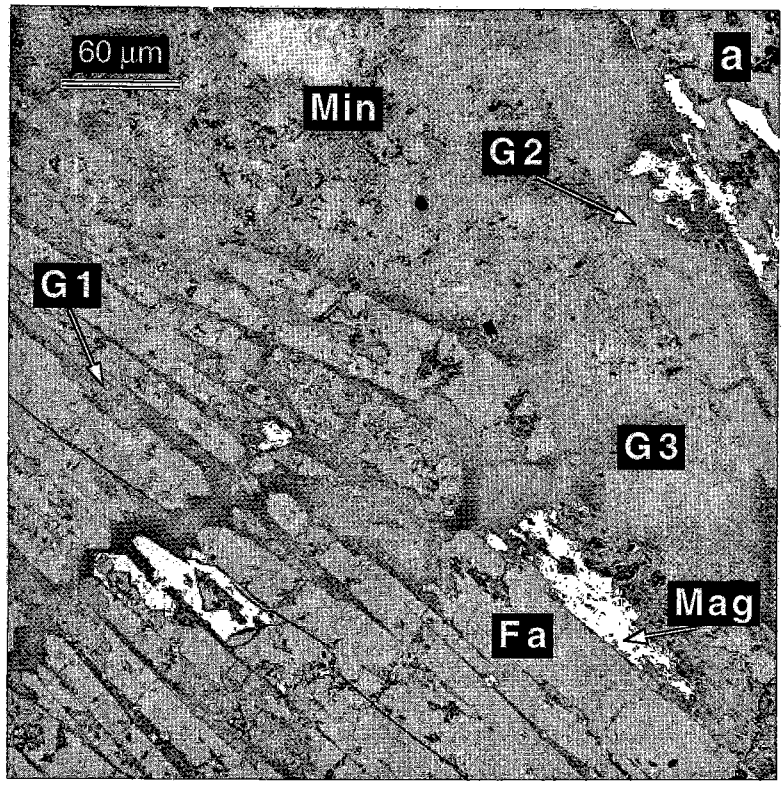

FIG. 3. Back-scattered electron images of fayalite (Fa) – greenalite (Gre) – minnesotaite (Min) assemblages in magnetite-rich ore of the Overlook gold deposit. G1: interstitial greenalite, G2: pseudomorphic greenalite, G3: matrix greenalite. a. Progressive development of greenalite from interstitial to pseudomorphic and matrix textures in sample 30–720. Note coarse Min replacing matrix Gre.

set in a matrix of an optically poorly resolved mixture of greenalite and minnesotaite, surrounded by patchily distributed coarser minnesotaite, quartz, magnetite, pyrrhotite, and calcite. Grunerite has been looked for, but not found. The chemographic relationships and low-pressure – low-temperature compatibilities among these minerals are shown projected in the ternary system FeO–SiO_2–H_2O (FSH) in Figure 5.

The FSH minerals clearly represent a paragenetic sequence as, taken together, they are too numerous to represent a frozen equilibrium. The distribution of the minerals, their textures, and their compositions (discussed below) are consistent with the passage of large amounts of an evolving hydrothermal fluid. Although the textural relations of fayalite and much of the calcite now present are ambiguous, it is believed likely that the fayalite formed by replacement of carbonate minerals (as at the Bluebell mine) in a carbonate – magnetite – sulfide rock, and that much of the remaining interstitial carbonate was subsequently replaced by greenalite and, later, by minnesotaite. Growth of this interstitial greenalite preserved the crystal faces of fayalite; in other words, for a time it may be inferred that fayalite and greenalite were in equilibrium. A later generation of greenalite partially replaced the fayalite. Further infiltration of hydrothermal fluid partially converted interstitial greenalite to minnesotaite, and a similar mixture of greenalite and minnesotaite (pale green in thin section) invaded the fayalite blades (or the pseudomorphic greenalite) and formed in matrix areas outside the nests of fayalite. Typically, little or nothing is left of the fayalite, but the distinctive subparallel or semiradiating texture of prisms is preserved in several samples by combinations of the pseudomorphic minerals greenalite, magnetite, pyrrhotite, ilvaite, and "iddingsite". Greenalite-free, somewhat coarser grains of minnesotaite and quartz appear to have coexisted in textural equilibrium and represent a late stage in the evolution of the hydrothermal fluid.

The composition of the fayalite as determined with the JEOL 733 microprobe at the University of

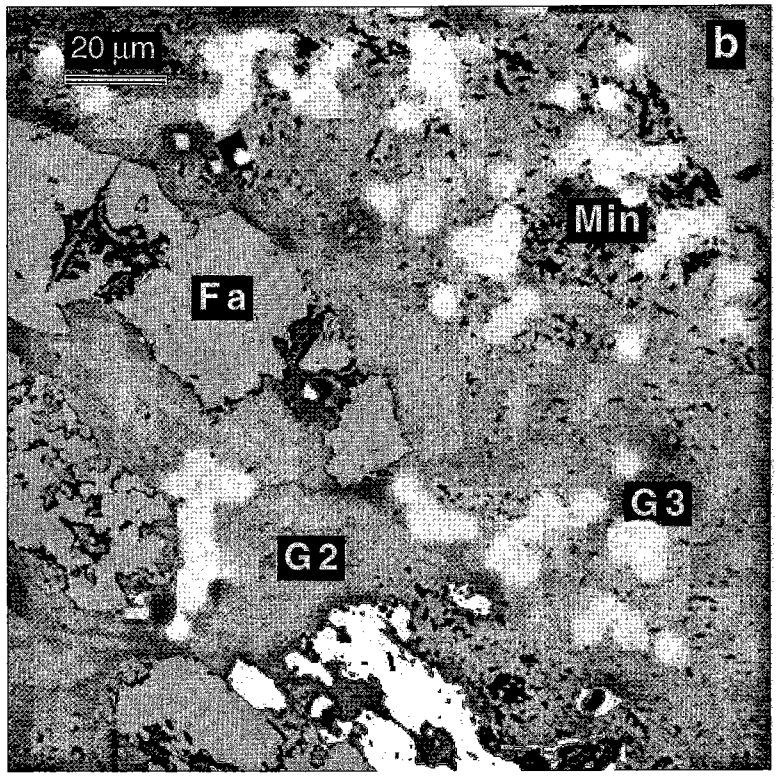

FIG. 3. Back-scattered electron images of fayalite (Fa) – greenalite (Gre) – minnesotaite (Min) assemblages in magnetite-rich ore of the Overlook gold deposit. G1: interstitial greenalite, G2: pseudomorphic greenalite, G3: matrix greenalite. b. Magnified part of a.

Washington varies slightly among three samples, but is homogeneous within samples and consistently very Fe-rich (Table 1). In terms of end-members, expressed in mole percent, fayalite lies in the range 95 to 98%, forsterite 1.5 to 3.0%, tephroite 0.15 to 2.1%, and larnite 0 to 0.2%.

The predominant serpentine mineral is greenalite, as determined by powder X-ray diffraction (XRD) and from the proportions of Si to *M* (where *M* = Fe + Mg + Mn), that is, Si/(Si + *M*) = $X_{Si} \approx 0.428$ (Guggenheim *et al.* 1982). The greenalite occurs in three textural settings with respect to the fayalite: "interstitial", "pseudomorphic", and "matrix" (Figs. 3, 4), although the chemical and textural character of interstitial and matrix areas tends to be continuous on the microprobe scale. The gradation from interstitial to matrix greenalite corresponds to greater admixture with minnesotaite (see below). Microprobe analyses, conducted using an electron beam 3 µm in diameter, show that the *interstitial* "greenalite" has values of X_{Si} in the range 0.43 to roughly 0.50 (Fig. 4), indicating that it is a mixture of greenalite and varying amounts of minnesotaite (X_{Si} = 0.571: Guggenheim & Eggleton 1986). Anhydrous analytical totals vary in a corresponding manner, from ~88.0 to ~92.0%; the X_{Mg} [Mg/(Mg + Fe + Mn)] suggests that greenalite, with X_{Mg} = 0.05, is mixed with minnesotaite with X_{Mg} = 0.14. The *pseudomorphic* greenalite has X_{Si} values tightly restricted to 0.43 to 0.45 (Table 2, Fig. 4), which means that it contains little, if any, admixed minnesotaite. Anhydrous totals average 88.5%, and the X_{Mg} equals 0.05, which is distinctly higher than the original olivine (0.015 to 0.03). The *matrix* material yielded no spot analyses that could be interpreted as 100% greenalite, but instead the analyses define a curved mixing trend (Fig. 4) extending from the "interstitial" greenalite to a minnesotaite end-member of composition X_{Mg} = 0.30 and 95% analytical total (anhydrous basis). XRD analysis of the matrix material with a Gandolfi camera by S. Guggenheim and R. Skirrow at Australian National University (S. Guggenheim, written commun., May 1991; see also Guggenheim & Eggleton 1998) confirmed that the matrix is a mixture of minnesotaite and greenalite. The overall curved mixing trend for interstitial and matrix material (Fig. 4) may be interpreted in at least two ways: (1) it represents the progressive replacement of greenalite by minnesotaite due to infiltration by a hydrothermal fluid evolving to higher Si and Mg contents, or (2) much of the interstitial greenalite is a mixed-layer composite

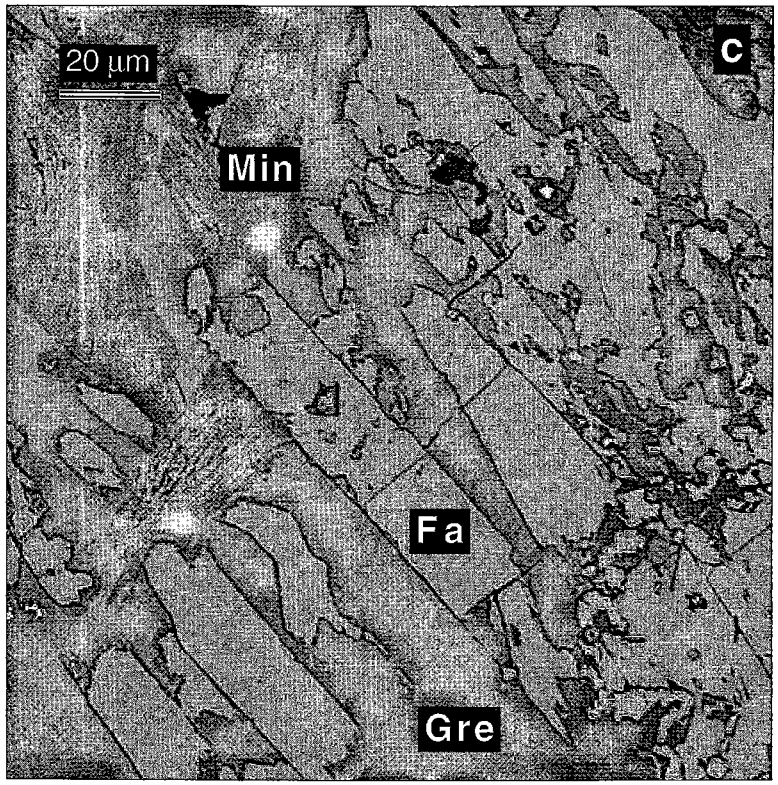

FIG. 3. Back-scattered electron images of fayalite (Fa) – greenalite (Gre) – minnesotaite (Min) assemblages in magnetite-rich ore of the Overlook gold deposit. G1: interstitial greenalite, G2: pseudomorphic greenalite, G3: matrix greenalite. c. Cross-cutting phases in sample 9–660 demonstrating the progression Fa to Gre to Min.

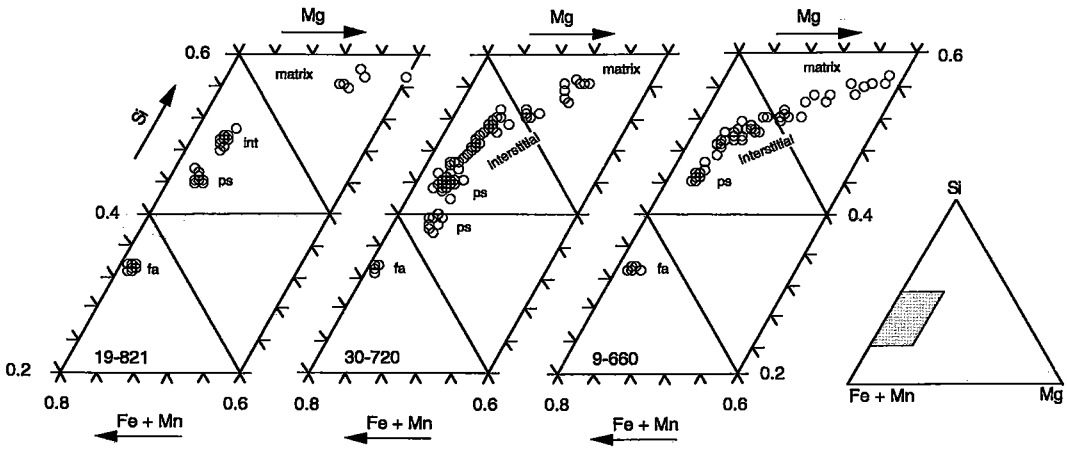

FIG. 4. Mineral compositions projected into the ternary system Si – (Fe + Mn) – Mg. Hydrothermal replacement minerals fayalite (fa), greenalite or iron serpentine pseudomorphs (ps) after fayalite, interstitial greenalite (int), and matrix mixtures of greenalite and minnesotaite.

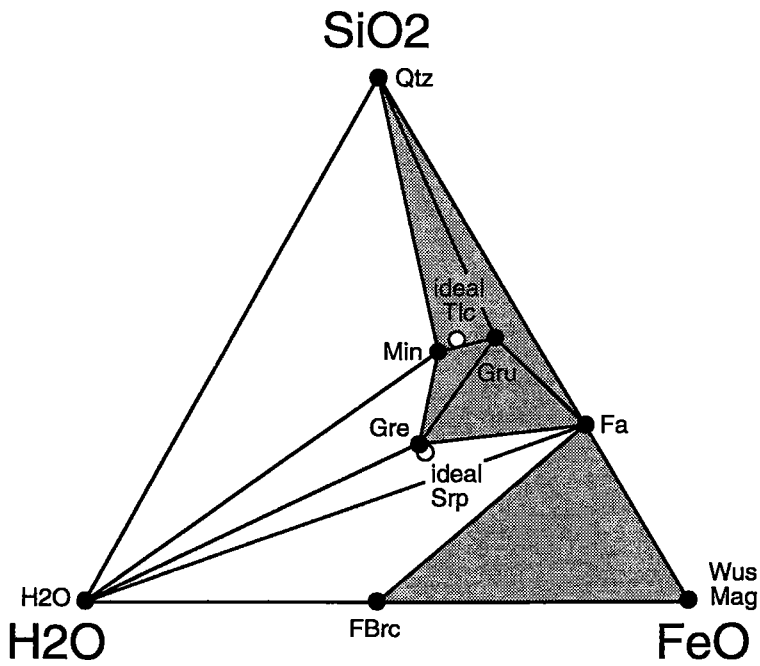

FIG. 5. Mineral compatibilities in the system FeO–SiO_2–H_2O at ~1 kbar and ~300°C. Filled circles denote phases in the system FSH, and open circles, ideal compositions in the system MSH. Shaded areas represent assemblages undersaturated in H_2O. Abbreviations after Kretz (1983); Min: minnesotaite, Gre: greenalite, FBrc: iron analogue of brucite.

TABLE 1. COMPOSITION OF OLIVINE AND ILVAITE, OVERLOOK GOLD DEPOSIT, WASHINGTON

Sample no.	30-720	9-660	19-821	30-720	9-660
Spots analyzed	5	14	8	3	1
SiO_2	29.44	29.45	29.29	28.84	29.40
Al_2O_3	0.00	0.02	0.00	0.00	0.00
FeO**	70.03	67.76	69.37	53.07	51.15
MnO	0.22	1.38	0.61	0.28	0.91
MgO	0.66	1.11	0.88	0.14	0.10
CaO	0.07	0.09	0.04	13.31	13.20
Total	100.42	99.81	100.19	95.67	94.76
			Atomic proportions*		
Si	0.992	0.994	0.989	1.968	2.022
Al	0.000	0.001	0.000	0.000	0.000
Fe	1.974	1.912	1.959	3.029	2.943
Mn	0.006	0.040	0.017	0.016	0.052
Mg	0.033	0.056	0.044	0.014	0.010
Ca	0.002	0.003	0.002	0.973	0.973
%fa	98.0	95.1	96.9		
%tep	0.3	2.0	0.8		
%fo	1.6	2.8	2.2		
%la	0.1	0.1	0.1		

The electron-microprobe analyses were carried out at the University of Washington, Seattle, with a JEOL 733 instrument operated at the following conditions: 15 kV, 10 nA current at the Faraday cup, beam diameter 3 μm, integration times 10 to 40 seconds, natural minerals as standards, and the correction factors of Armstrong (1988). The compositions are expressed in wt.% oxides. * Basis of recalculation: olivine: four atoms of oxygen: ilvaite: six cations. ** Total Fe expressed as FeO.

of greenalite and minnesotaite; the X_{Mg} of the minnesotaite interlayers may for crystal-structure reasons be lower than the physically separate minnesotaite, hence the curved or "dog-leg" nature of the mixing trend. The coarser grain-size of the sheet silicates in sample 19–821 allowed a clearer distinction between interstitial greenalite and matrix minnesotaite.

In sample 30–720, some of the pseudomorphic serpentine was found to possess a set of distinctly lower X_{Si} values, from 0.38 to 0.40 (Table 2, Fig. 4). This composition would seem to correspond to an iron analogue of ideal serpentine $Mg_3Si_2O_5(OH)_4$, in other words a possible iron analogue of lizardite or iron analogue of chrysotile (the Ni analogues are known as the minerals népouite and pecoraite). Both types of pseudomorphic serpentine, the greenalite and the iron serpentine, have anhydrous analytical totals in the range 88 to 89%. The iron serpentine and greenalite are intergrown on a scale barely resolvable by electron microprobe, and minnesotaite is absent from these intergrowths. Possibly this apparently rare alteration of fayalite to iron-rich serpentine rather than greenalite reflected a local fluid of lower silica activity, perhaps an earlier fluid. Thus, the iron serpentine and greenalite

TABLE 2. COMPOSITION OF SERPENTINE AND GREENALITE PSEUDOMORPHS, AND MINNESOTAITE, OVERLOOK GOLD DEPOSIT, WASHINGTON

	Fe-serp. pseud.	greenalite pseudomorphs			minnesotaite		
Sample no.	30-720	30-720	9-660	19-821	30-720	9-660	19-821
Spots analyzed	18	34	16	12	11	3	6
SiO_2	31.44	35.32	36.82	35.75	52.61	53.65	50.50
Al_2O_3	0.01	0.00	0.05	0.03	0.10	0.06	0.15
FeO	54.51	51.25	49.88	50.55	34.80	29.46	35.09
MnO	0.08	0.22	0.94	0.67	0.04	0.08	0.25
MgO	2.38	1.79	1.78	1.76	7.82	11.19	7.67
CaO	0.08	0.10	0.11	0.07	0.05	0.02	0.04
H_2O*	9.61	9.98	10.20	10.03	5.58	5.68	5.43
Total	98.21	98.67	99.78	98.86	101.00	100.13	99.12
Atomic proportions							
Si	1.962	2.123	2.166	2.137	3.957	3.966	3.904
Al	0.001	0.000	0.004	0.002	0.009	0.005	0.014
Fe	2.845	2.576	2.454	2.527	2.189	1.821	2.269
Mn	0.004	0.011	0.047	0.034	0.002	0.005	0.016
Mg	0.221	0.161	0.156	0.157	0.877	1.233	0.884
Ca	0.005	0.006	0.007	0.005	0.004	0.002	0.003

The electron-microprobe analyses were carried out as described in Table 1. The compositions are expressed in wt.% oxides.
* The proportion of H_2O was calculated assuming the structural formulas of serpentine, greenalite and minnesotaite. Total Fe is expressed as FeO.

here may be analogous to the magnesian serpentines, antigorite and chrysotile, in the sense of having an inferred temperature-range of stable coexistence of the two species (Evans *et al.* 1976). Further characterization of the iron serpentine by TEM is planned.

Nests of nearly greenalite-free minnesotaite occur in parts of the matrix in the fayalite-bearing rocks (Fig. 3c). Electron-microprobe analyses (Table 2) show X_{Si} values close to 0.57 and X_{Mg} ranging up to as much as 0.46. Next to quartz, the minnesotaite is free of greenalite.

We infer the red "iddingsite" pseudomorphic replacement of fayalite to be very late in the alteration sequence. It appears to be predominantly a ferric-iron-bearing material, giving consistent electron-microprobe analyses with X_{Si} in the range 0.50 to 0.55. Its X_{Mg} is smaller than the greenalite and is identical to that of the fayalite; it contains variable amounts of Ca (0.4 to 1.3% CaO), Na (0 to 0.6% Na_2O), and traces of K. The X_{Si} corresponds neither to a 2:1 sheet silicate (talc–pyrophyllite type) nor to a trioctahedral 1:1 serpentine, but suggests instead a dioctahedral 1:1 sheet silicate with the composition $Fe^{3+}{}_2Si_2O_5(OH)_4$, which would be a ferric iron analogue of kaolinite. The presence of shrinkage cracks on the polished section and anhydrous analysis totals that have varied from 91 to 82% over time suggest that it is a ferrian analogue of a halloysitic type of clay mineral, capable of accommodating variable amounts of absorbed interlayer H_2O, and large-radius cations. Additional characterization work by TEM is in progress.

Fluid Inclusions

Two-phase, apparently primary H_2O inclusions in the calcite matrix to fayalite and in late quartz provide a means of bracketing the sequence and hence possible

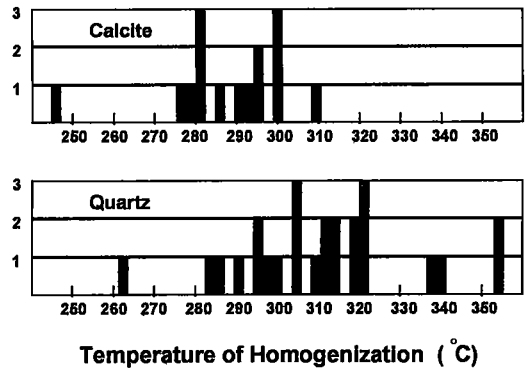

FIG. 6. Histograms of homogenization temperatures (T_H) of fluid inclusions. Upper chart displays T_H of fluid inclusions in calcite locally replaced by iron silicate minerals; lower chart contains T_H values from inclusions in quartz that overprints the iron silicate assemblages.

temperature of formation of the iron-rich silicates including the fayalite. The small size of the inclusions (<15 μm), the presence of abundant metalliferous microscopic and submicroscopic "debris", and a high density of annealed and unannealed fractures rendered impossible any sort of reliable freezing–heating measurements in either calcite or quartz, and made it difficult to distinguish primary from other types of inclusions. On the other hand, liquid–vapor homogenization measurements were possible. As illustrated in Figure 6, 14 of 15 heating measurements in calcite believed to have preceded crystallization of fayalite + greenalite indicate homogenization temperatures from 280 to 310°C , and 20 of 25 measurements in quartz that crystallized after fayalite + greenalite indicate

temperatures between 280 and 320°C; those above 320°C are possibly due to the entrapment of two-phase fluids, although other evidence of boiling is absent. Many of the inclusions are large and unambiguously primary in appearance.

Oxygen Isotope Thermometry

Measurement of the fractionation of oxygen isotopes between quartz and late magnetite, both of which on textural grounds formed after the fayalite, provide an additional constraint on temperature. Two samples of quartz and magnetite from different size-fractions of fayalite-bearing sample OLC 30–720 were separated by magnetic methods and analyzed for $^{18}O/^{16}O$ following the methods of Clayton & Mayeda (1963). The purity of quartz fractions was estimated at 99%, and that of magnetite, at 95–98% (H. Krueger, written commun., 1992). Results relative to SMOW were: quartz $\delta^{18}O = 16.85 \pm 0.5‰$ and magnetite $\delta^{18}O = -3.0 \pm 0.6‰$, thus $\Delta^{18}O = 19.85 \pm 0.65‰$. This value indicates an equilibrium temperature of fractionation of about 280 ± 10°C (Matthews *et al.* 1983) or 290 ± 6°C (Chiba *et al.* 1989). Because textural evidence suggests a protracted period of post-fayalite crystallization of magnetite and quartz, these determinations of temperature may be questionable in light of the possible paragenetic separation of quartz and magnetite. Nevertheless, they are consistent with those obtained from the fluid inclusions. Furthermore, there are no indications from any source of substantially higher temperatures at the time of fayalite growth.

Barometry

Possible metamorphic pressure exerted on the massive sulfide portions of the Overlook orebody was recorded by the FeS content of sphalerite in equilibrium with pyrite and pyrrhotite, using the equations of Toulmin & Barton (1964) and the method of Scott (1973) and Hutchinson & Scott (1981). Measurements of X_{FeS} by electron microprobe on 24 grains of sphalerite in textural equilibrium with pyrite and pyrrhotite (Rasmussen 1993) showed a mean value of 19.77 mole %, from which we infer $P_{max} = 0.77 \pm 0.3$ kbar. A rounded-off estimate of one kbar is adopted in some of the phase-equilibrium diagrams that follow.

Phase Equilibria

Low-temperature, low-pressure phase relations in the system $FeO–SiO_2–H_2O$ (FSH) can be expected to differ from those in the much more thoroughly studied system $MgO–SiO_2–H_2O$ (MSH), as the FSH sheet silicates minnesotaite and greenalite take the place of their MSH counterparts talc and antigorite or chrysotile. The exchange of Fe for Mg is accompanied by an increasing degree of size misfit between the layers of tetrahedra and octahedra in the sheet silicates, and, although this problem is alleviated by the development of modulated structures (Guggenheim & Eggleton 1988), the stabilities of the sheet silicates are nevertheless diminished.

TABLE 3. THERMODYNAMIC PROPERTIES OF END-MEMBER FSH MINERALS

	Fayalite[1] Fe_2SiO_4	Grunerite[2] $Fe_7Si_8O_{22}(OH)_2$	Minnesotaite[3] $Fe_3Si_4O_{9.6}(OH)_{2.8}$	Greenalite[4] $Fe_{2.8}Si_{2.1}O_5(OH)_4$
ΔH^o_f (kJ)	-1479.360	-9623.3	-4941.2	-3333.0
S^o (J/K)	150.93	725	378	311.62
V^o (J/bar)	4.630	27.84	15.34	11.98
k_0	248.93	1347.83	731.09	612.70
$k_1 \times 10^{-2}$	-19.239	-93.5691	-55.05	-51.79
$k_2 \times 10^{-5}$	0.0	-202.285	-101.142	-53.10
$k_3 \times 10^{-7}$	13.910	303.919	159.838	96.06
$v_1 \times 10^6$	-0.7300	-1.6703	-1.6999	-1.8103
$v_2 \times 10^{12}$	0.0	8.68919	5.665	4.5243
$v_3 \times 10^8$	26.546	28.400	29.447	27.151
$v_4 \times 10^{10}$	79.482	0.0	0.0	67.35

Sources of data: 1 Berman (1988), 2 Ghiorso *et al.* (1995), 3 Lattard & Evans (1992), 4 this work. Note: $Cp = k_0 + (k_1/T) + (k_2/T^2) + k_3/T^3)$ J/K; $V/V^o = 1 + v_1(P - P_r) + v_2(P - P_r)^2 + v_3(T - T_r) + v_4(T - T_r)^2$ J/bar.

Thermodynamic data are available for the minerals fayalite, ferrosilite (Berman 1988, and references therein), grunerite (Ghiorso *et al.* 1995), and minnesotaite (Evans & Guggenheim 1988, Lattard & Evans 1992). Some rough constraints on the thermodynamic properties of greenalite may be derived from diverse sources, as follows. First, we adopt an average end-member formula of $Fe_{2.8}Si_{2.1}O_5(OH)_4$ based on natural greenalite (Guggenheim *et al.* 1982). The cell dimensions of Sierra de Cartagena greenalite (391 Å^3: Guggenheim *et al.* 1982) may be extrapolated and converted to an end-member molar volume of 119.8 cm^3; a 298 K entropy is estimated after the method of Holland (1989), and heat-capacity coefficients, after Berman & Brown (1985). The 298 K enthalpy may be constrained from the following: (1) greenalite from Sierra de Cartagena (mole fractions Fe = 0.84, Mg = 0.13, Mn = 0.03) was successfully reacted to fayalite (Fe = 0.92, Mg = 0.08) + quartz + H_2O (a metastable reaction) in 46 days at 415°C and 2 kilobars in a cold-seal rod bomb in reconnaissance experimental work in 1981 at the University of British Columbia by B.W. Evans and M. Engi (unpublished); (2) no grunerite formed in the Overlook deposit, from which we infer that the grunerite terminal reaction: greenalite + minnesotaite = grunerite + H_2O exceeds 300°C for the compositions of Overlook greenalite (~95% Fe end-member) and minnesotaite (~86% Fe end-member), thereby permitting the paragenetic sequence at Overlook (Fa + Gre → Gre + Min → Min + Qtz) to exclude grunerite, and (3) the reaction: greenalite + quartz = minnesotaite + H_2O in contact-metamorphosed banded iron-formation proceeds at about 150°C, an average based on several field studies, as reviewed, for example, in Miyano (1978). The thermodynamic data adopted for these FSH minerals, consistent with those of Berman (1988), including *very provisional* values

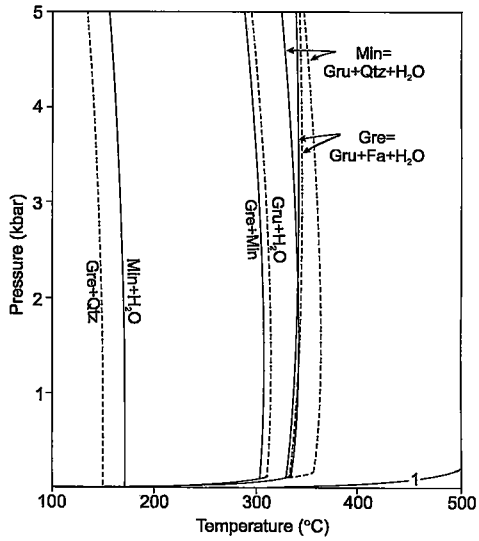

FIG. 7. Calculated P–T phase diagram of the system FeO–SiO_2–H_2O at low temperatures. Full lines, pure FSH phases; dashed lines, Overlook compositions (see text). Reaction 1: Gru = Fa + Qtz + H_2O. Abbreviations as in Figure 5.

for greenalite, are given with their sources in Table 3. These data predict the metastable reaction of Sierra de Cartagena greenalite to fayalite + quartz + H_2O to be at about 380°C at 2 kilobars.

A P–T phase diagram showing relationships in the system FeO–SiO_2–H_2O among fayalite, greenalite, grunerite, minnesotaite, quartz, and H_2O calculated using these thermodynamic data and GEØ–CALC software (Brown *et al.* 1988) is given in Figure 7. The T – X_{Si} diagrams of Figure 8 and the T – μ_{FeMg-1} diagram of Figure 9 permit visualization of the basic differences in phase relationships between the FSH and MSH systems under conditions of H_2O saturation. Figures 8, 9, and 10 are constructed for a pressure of 1 kilobar; in the range 0.5 to 3 kbar, pressure has little effect on the temperature of the reaction curves. The diminished stability especially of talc (relative to amphibole, quartz, and H_2O), caused by an increase in μ_{FeMg-1}, results in an isobaric invariant point [Opx,Qtz] in the system FMSH (Fig. 9) where serpentine, talc or minnesotaite, FeMg-amphibole, olivine, and H_2O coexist. This isobaric invariant point corresponds to the H_2O-conserved reaction: olivine + talc or minnesotaite = MgFe-amphibole + serpentine; the left-hand side of this reaction is stable in Mg-rich systems such as meta-

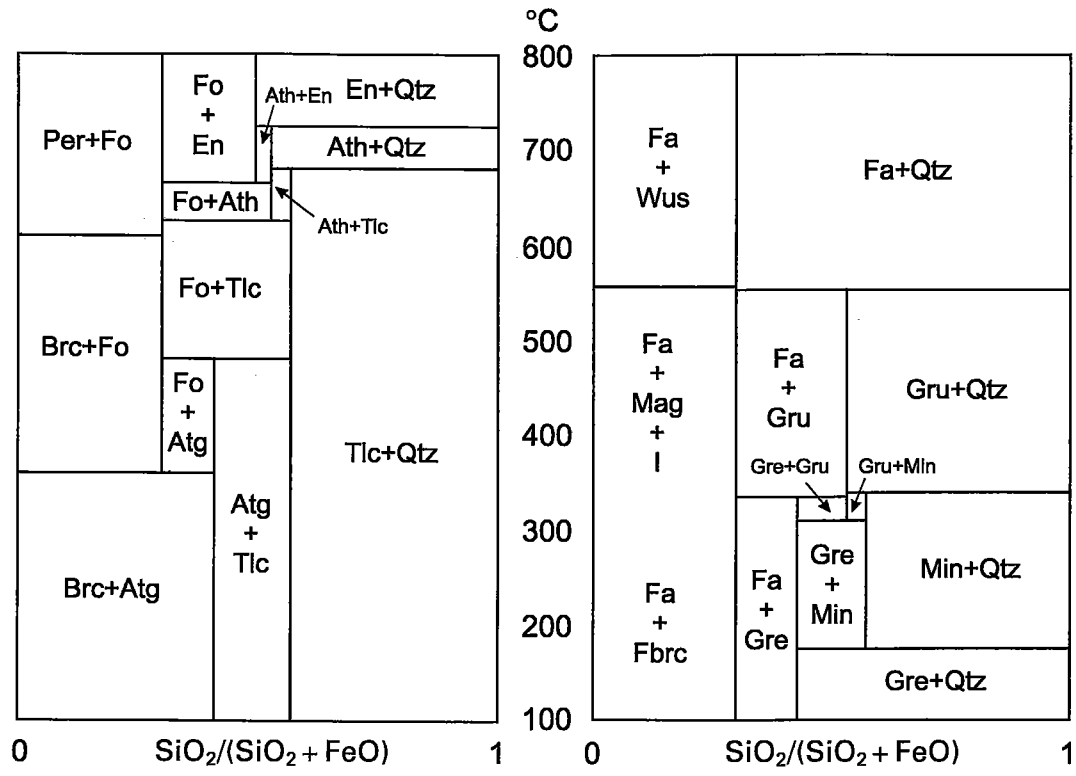

FIG. 8. A comparison of the MSH and FSH systems in isobaric (1 kbar, H_2O-saturated) T–$X(SiO_2)$ diagrams. Abbreviations as in Figure 5; I: iron, FBrc: iron analogue of brucite.

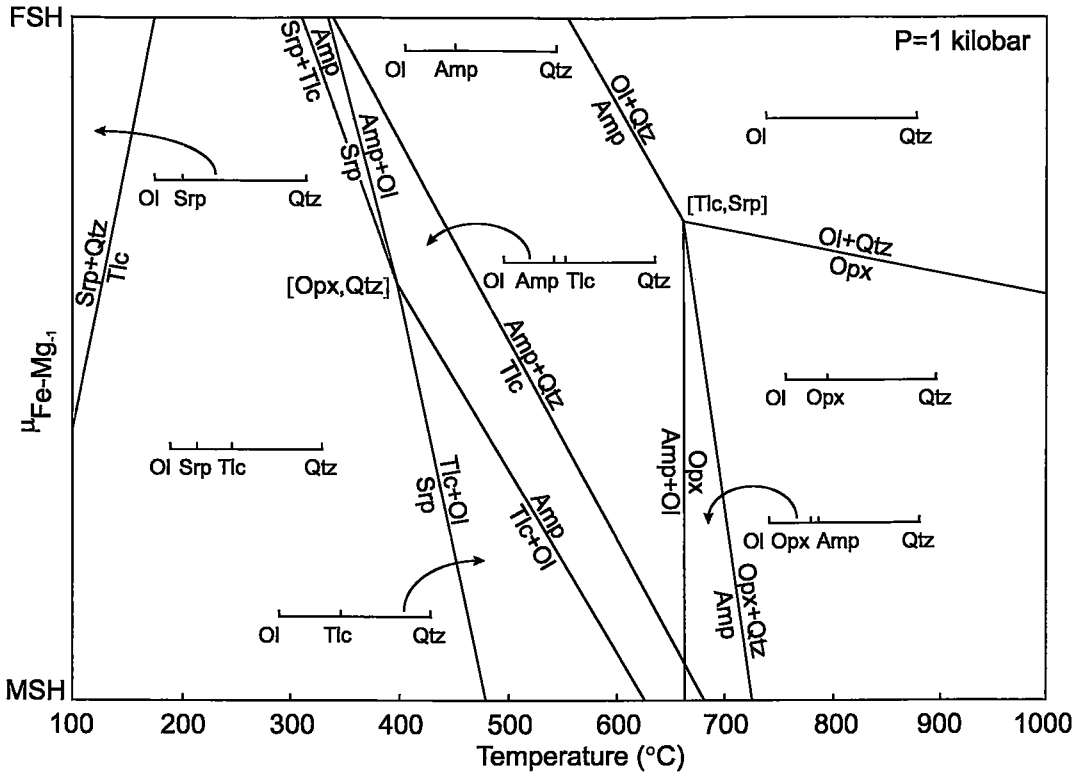

FIG. 9. T – $\mu FeMg_{-1}$ for the system FMSH at 1 kilobar, H_2O-saturated. Mineral abbreviations as in Figure 5; Srp: antigorite or greenalite, Amp: anthophyllite or grunerite. The straight-line relationships are a first approximation to what are in many cases equilibria with both first- and second-order transitions among the minerals, and slightly changing stoichiometry.

morphosed ultramafic rocks, whereas the right-hand side is stable in Fe-rich systems such as hydrothermal deposits and, potentially, quartz-free meta-ironstones. These changes in compatibilities are consistent with shifts due to the mass-action law according to the relative Fe:Mg ratios of the minerals in exchange equilibrium. To eliminate the invariant point, and render phase relations in FSH topologically the same as in MSH (*e.g.*, Yoder 1957, Burt 1972) would require the upper stability limit of greenalite to have been overestimated here by approximately 90°C; this would rule out greenalite at Overlook at 300°C. Whereas in the system MSH, the stability limit of talc exceeds that of serpentine (antigorite) by some 200°C, in the system FSH, according to our calculations, the upper thermal limits of minnesotaite and greenalite are nearly identical (Figs. 7, 8, 9). Conditions of silica undersaturation are basic in extending the stabilities of fayalite (down-temperature) and greenalite (up-temperature).

A possible oxygen-conserved, low-temperature terminal reaction for fayalite in the FSH system (Fig. 8, to greenalite + the iron analogue of brucite?) has not yet been established.

Added to Figures 7 and 10 are equilibrium curves displaced from their FSH locations according to the typical (X_{Fe}) compositions of minerals at Overlook, namely: olivine Fa 0.98, Gru 0.93 (estimated from Mg/Fe partitioning data, Ghiorso *et al.* 1995), Min 0.86, Gre 0.95, adopting Raoult's Law activities for internal consistency in the absence of activity–composition data for minnesotaite and greenalite. According to these calculations, greenalite + minnesotaite is more stable than grunerite + H_2O for Overlook compositions at temperatures below 315°C, assuming a pressure of 1 kilobar. Increasing Mg:Fe ratios raise this temperature limit. In addition, the assemblage fayalite + greenalite is stable below 340°C, this being the low-temperature limit for fayalite + grunerite + H_2O (Figs. 7, 9). Between ~170°C and 315°C, fayalite, greenalite, minnesotaite, and quartz constitute the binary anhydrous FeO–SiO_2 chemography (Fig. 9), permitting this paragenetic sequence to be realized isothermally in the

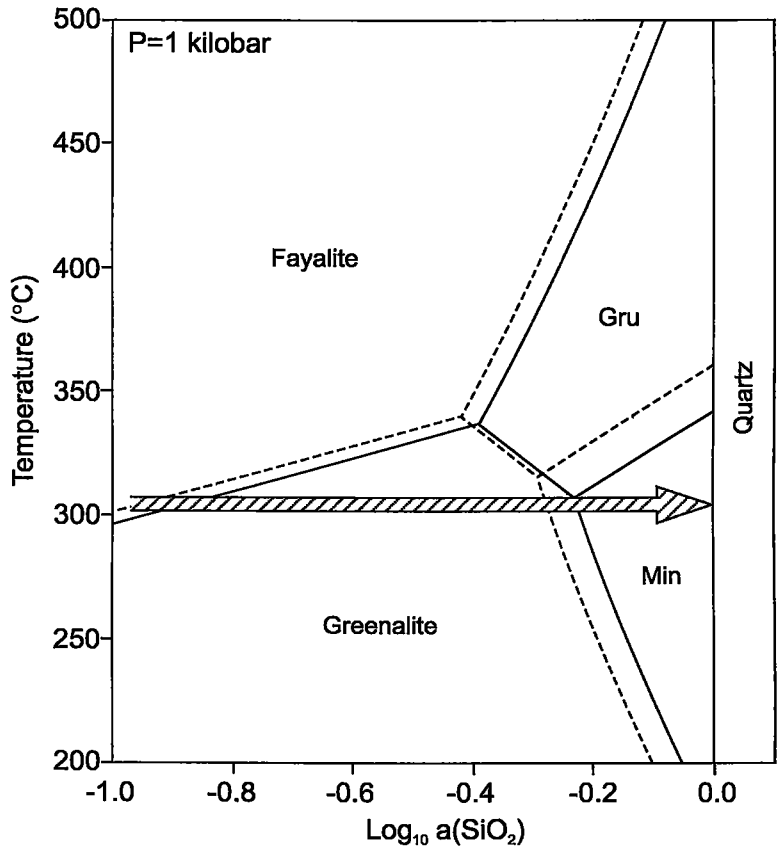

FIG. 10. T – log $a(SiO_2)$ diagram for the system FSH at 1 kilobar, H_2O-saturated. Quartz standard state. Full lines, pure FSH phases; dashed lines, Overlook compositions. Arrow is inferred change in fluid composition at Overlook.

T – $a(SiO_2)$ diagram (Fig. 10) as a result of infiltration by an increasingly SiO_2-rich hydrothermal fluid. At Overlook, the quartz–magnetite isotope-inferred temperatures and the inclusion homogenization temperatures suggest a temperature close to 300°C for this event. Maintenance of these mineral assemblages requires, of course, that the fluid be extremely reducing, with log $f(O_2)$ at 300°C less than QFM conditions of –35.7 (Frost 1991), or even lower, since $a(SiO_2) < 1$. The alteration of fayalite to "iddingsite" is a totally separate event recording the subsequent introduction of much more oxidizing, near-surface meteoric fluids.

ORIGIN OF IRON SILICATES AT THE OVERLOOK OREBODY

Fayalite and related iron-rich silicates are interpreted to be the product of hydrothermal alteration of a carbonate-bearing rock at a temperature of ~300°C. The presence of calcite implies a certain minimum, but extremely low, CO_2-activity in the fluid at the site of alteration, much lower, as calculations would suggest, than the CO_2-activity needed to stabilize siderite rather than fayalite. The fluid must initially have been very SiO_2-poor and very reduced. Texturally later greenalite, minnesotaite, and quartz comprise a paragenetic sequence corresponding to increasing SiO_2 in the infiltrating fluid. Temperature – activity (SiO_2) relations in the FSH system, with allowance for minor Mg, permit this sequence to form isothermally at 300°C and a pressure of about a kilobar (Fig. 10). In this metasomatic environment, the coexistence of fayalite with greenalite, and of greenalite with minnesotaite, is possible only at specific values of SiO_2-activity, at constant T, P, and $a(H_2O)$. Such conditions may have been of some duration, depending on the rate of influx

of silica in solution. The model reactions involved are:

$$\underset{\text{Fa}}{14\ Fe_2SiO_4} + 7\ (SiO_2)_{aq} + 20\ H_2O = \underset{\text{Gre}}{10\ Fe_{2.8}Si_{2.1}O_5(OH)_4} \quad (1)$$

$$\underset{\text{Gre}}{150\ Fe_{2.8}Si_{2.1}O_5(OH)_4} + 245\ (SiO_2)_{aq} = \underset{\text{Min}}{140\ Fe_3Si_4O_{9.6}(OH)_{2.8}} + 104\ H_2O \quad (2)$$

The growth of minnesotaite, and possibly also the greenalite, was accompanied by an increase in the Mg:Fe ratio of the introduced fluid. In this respect, our hydrothermal paragenetic sequence differs from that expected in the alteration of fayalite in pegmatites to low-temperature hydrous iron silicates (*e.g.*, Janeczek 1989).

Ilvaite is likely to have formed as a consequence of the enrichment in the pore fluid of SiO_2 or increase in H_2O/CO_2, or both, according to the oxygen-conserved reaction:

$$\underset{\text{Fa}}{3\ Fe_2SiO_4} + \underset{\text{Mag}}{2\ Fe_3O_4} + \underset{\text{Cal}}{4\ CaCO_3} + 5\ (SiO_2)_{aq} + 2\ H_2O = \underset{\text{Ilv}}{4\ CaFe_3Si_2O_8(OH)} + 4\ (CO_2)_{aq} \quad (3)$$

An oxidation reaction at $f(O_2)$ below the QFM buffer, in the absence of magnetite, would achieve the same result. Later, the fluid became more oxidizing, as magnetite replaced parts of the fayalite.

Fluids typical of Tertiary extensional regimes in the Canadian Cordillera are characterized by meteoric oxygen and hydrogen isotopic signatures, and low salinity (Nesbitt & Muehlenbachs 1989a, b). Studies of quartz separated from the Overlook quartz veins are consistent with these characteristics (Rasmussen 1993). Despite their meteoric origin, the hydrothermal fluids at Overlook that produced the silicate prageneses described here had oxygen fugacities at or below the QFM buffer curve. This calls for a prolonged history of crustal circulation and an opportunity for the fluid to undergo a major change in redox state. Textural evidence for the conversion of pyrrhotite and pyrite to magnetite in brecciated massive ore zones at Overlook (Rasmussen 1993) suggests a possible mechanism for depleting the invading fluid of oxygen. The acidic fluid so formed would instantly target calcite for solution and replacement, and at 300°C the log $f(O_2)$ of the fluid would have been less than or equal to –35, corresponding to the coexistence of magnetite, pyrite, and pyrrhotite (Bowers *et al.* 1984), practically identical to the QFM buffer.

Acknowledgements

This work represents a portion of the first author's doctoral research at the University of Washington, supervised by E.S. Cheney; we thank E.S. Cheney for reviewing parts of this paper. The project was supported by GSA Student Research Grant #4776–91 and two research assistantships (#62–5414 and #62–5437) from the Washington Mining and Minerals Resources Research Institute in 1988 and 1989. Echo Bay Mines, Ltd. generously provided materials, access to Overlook core and underground workings, and permission to publish the Overlook data. Particular recognition is extended to S. Guggenheim and R. Skirrow for XRD determination of matrix iron silicates at the Australian National University, Canberra. Martin Engi is thanked for assistance in the experimental work on greenalite. We thank the Associate Editor, J.F. Slack, and two reviewers, particularly I.C.W. Fitzsimons, for constructive critical comments. Evans thanks NSF for support under grant EAR93–03972.

References

Alpers, C.N. (1980): *Mineralogy, paragenesis, and zoning of the Luz vein, Uchucchacua, Peru.* B.A. thesis, Harvard Univ., Cambridge, Massachusetts.

Archibald, D.E. (1996): $^{40}Ar/^{39}Ar$ dating of sericitic alteration from the Lamefoot deposit. Unpubl. rep., Echo Bay Minerals Co.

Armstrong, J.T. (1988): Bence–Albee after 20 years: review of the accuracy of alpha-factor correction procedures for oxide and silicate minerals. *In* Microbeam Analysis, Applications in Geology (J.T. Armstrong, ed.). San Francisco Press, San Francisco, California.

Berman, R.G. (1988): Internally consistent thermodynamic data for minerals in the system Na_2O–K_2O–CaO–MgO–FeO–Fe_2O_3–Al_2O_3–SiO_2–TiO_2–H_2O–CO_2. *J. Petrol.* **29**, 445-522.

_____ & Brown, T.H. (1985): The heat capacity of minerals in the system Na_2O–K_2O–CaO–MgO–FeO–Fe_2O_3–Al_2O_3–SiO_2–TiO_2–H_2O–CO_2: representation, estimation, and high temperature extrapolation. *Contrib. Mineral. Petrol.* **89**, 168-183.

Birch, W.D. (1984): Roepperite from Broken Hill (New South Wales) is ferroan tephroite. *Mineral. Mag.* **48**, 137-139.

Bowers, T.S., Jackson, K.J. & Helgeson, H.C. (1984): Equilibrium activity diagrams for coexisting minerals and aqueous solutions at pressures and temperatures to 5 kb and 600°C. Springer-Verlag, New York, N.Y.

Brown, T.H., Berman, R.G. & Perkins, E.H. (1988): GEØ–CALC: software package for calculation and display of pressure – temperature – composition phase diagrams using an IBM or compatible personal computer. *Comput. Geosci.* **14**, 279-289.

BURT, D.M. (1972): The system Fe–Si–C–O–H: a model for metamorphosed iron formations. *Carnegie Inst. Wash., Year Book* **71**, 435-443.

CHENEY, E.S. & RASMUSSEN M.G. (1996): Regional geology of the Republic area. *Washington Geology* **24**(2), 3-7.

CHIBA, H., CHACKO, T., CLAYTON, R.N. & GOLDSMITH, J.R. (1989): Oxygen isotope fractionations involving diopside, forsterite, magnetite, and calcite: application to geothermometry. *Geochim. Cosmochim. Acta* **53**, 2985-2995.

CHURCH, B.N. (1986): Geology and mineralization in the Mount Attwood – Phoenix area, Greenwood, B.C. *B.C. Ministry of Energy, Mines, and Petroleum Resources, Pap.* **1986-2**.

CLAYTON, R.N. & MAYEDA, T.K. (1963): The use of bromine pentafluoride in the extraction of oxygen from oxide and silicates for isotopic analysis. *Geochim. Cosmochim. Acta* **27**, 43-52.

EVANS, B.W. & GUGGENHEIM, S. (1988): Talc, pyrophyllite, and related minerals. *In* Hydrous Phyllosilicates (S.W.Bailey, ed.). *Rev. Mineral.* **19**, 225-294.

_____, JOHANNES, W., OTERDOOM, H. & TROMMSDORFF, V. (1976): Stability of chrysotile and antigorite in the serpentinite multisystem. *Schweiz. Mineral. Petrogr. Mitt.* **56**, 79-93.

FOLEY, N.K., SLACK, J.F. & FLOHR, M.J.K. (1997) Fluid evolution and mineral deposition in the Bald Mountain volcanogenic massive sulfide deposit, northern Maine. *Geol. Soc. Am., Abstr. Programs* **29**(6), A-59.

FROST, B.R. (1991): Introduction to oxygen fugacity and its petrological importance. *In* Oxide Minerals: Petrologic and Magnetic Significance (D.H. Lindsley, ed.). *Rev. Mineral.* **25**, 1-9.

FYLES, J.T. (1990): Geology of the Greenwood – Grand Forks area, British Columbia. *B.C. Ministry of Energy, Mines and Petroleum, Open File* **1990-25**.

_____ (1995): Knob Hill Group, Attwood Group, and Brooklyn Formation. *Geol. Assoc. Can. – Mineral. Assoc. Can., Field Trip Guidebook* **B2**.

GHIORSO, M.S., EVANS, B.W., HIRSCHMANN, M.M. & YANG, H. (1995): Thermodynamics of the amphiboles: Fe–Mg cummingtonite solid solutions. *Am. Mineral.* **80**, 502-519.

GUGGENHEIM, S., BAILEY, S.W., EGGLETON, R.A. & WILKES, P. (1982): Structural aspects of greenalite and related minerals. *Can. Mineral.* **20**, 1-18.

_____ & EGGLETON, R.A. (1986): Structural modulations in iron-rich and magnesium-rich minnesotaite. *Can. Mineral.* **24**, 479-497.

_____ & _____ (1988): Crystal chemistry, classification, and identification of modulated layer silicates. *In* Hydrous Phyllosilicates (Exclusive of Micas) (S.W.Bailey, ed.). *Rev. Mineral.* **19**, 675-725.

_____ & _____ (1998): Modulated crystal structures of greenalite and caryopilite: a system with long-range, in-plane structural disorder in the tetrahedra sheet. *Can. Mineral.* **36**,

GUNNING, H.C. (1936): Knebelite at Bluebell mine, Kootenay Lake, B.C. *Trans. R. Soc. Can., Sect.* **IV**, 19-22.

HOLLAND, T.J.B. (1989): Dependence of entropy on volume for silicate and oxide minerals: a review and predictive model. *Am. Mineral.* **74**, 5-13.

_____ & POWELL, R. (1990): An enlarged and updated internally consistent thermodynamic dataset with uncertainties and correlations: the system K_2O–Na_2O–CaO–MgO–MnO–FeO–Fe_2O_3–Al_2O_3–TiO_2–SiO_2–C–H_2–O_2. *J. Metamorphic Geol.* **8**, 89-124.

HUTCHINSON, M.N. & SCOTT, S.D. (1981): Sphalerite geobarometry in the Cu–Fe–Zn–S system. *Econ. Geol.* **76**, 143-153.

JANECZEK, J. (1989): Manganoan fayalite and products of its alteration from the Strzegom pegmatites, Poland. *Mineral. Mag.* **53**, 315-325.

KRETZ, R. (1983) Symbols for rock-forming minerals. *Am. Mineral.* **68**, 277-279.

LATTARD, D. & EVANS, B.W. (1992): New experiments on the stability of grunerite. *Eur. J. Mineral.* **4**, 219-238.

LOWE, C.H. & LARSON, P.B. (1996): Geology of the Key East gold deposit, Ferry County, Washington. *In* Geology and Ore Deposits of the American Cordillera (A.R. Coyner & P.L. Fahey, eds.). *Geol. Surv. Nevada, Symp. Proc. (Reno–Sparks, Nevada)*, 1111-1132.

MATTHEWS, A., GOLDSMITH, J.R. & CLAYTON, R.N. (1983): Oxygen isotope fractionations involving pyroxenes: the calibration of mineral-pair geothermometers. *Geochim. Cosmochim. Acta* **47**, 631-644.

MIYANO, T. (1978): Phase relations in the system Fe–Mg–Si–O–H and environments during low-grade metamorphism of some Precambrian iron formations. *J. Geol. Soc. Japan* **84**, 679-690.

MONGER, J.W.H., PRICE, R.A. & TEMPELMAN-KLUIT, D.J. (1982): Tectonic accretion and the origin of the two major metamorphic and plutonic belts in the Canadian Cordillera. *Geology* **10**, 70-75.

_____, WHEELER, J.O., TIPPER, H.W., GABRIELSE, H., HARMS, T., STRUIK, L.C., CAMPBELL, R.B., DODDS, C.J., GEHRELS, G.E. & O'BRIEN, J. (1991): Cordilleran Terranes. *In* Geology of the Cordilleran Orogen in Canada (H. Gabrielse & C.J. Yorath, eds.). *Geol. Surv. Can., Geology of Canada* **4**, 281-327 (also *Geol. Soc. Am., The Geology of North America* **G-2**).

MOSSMAN, D.J. & PAWSON, D.J. (1976): X-ray and optical characterization of the forsterite – fayalite – tephroite series with comments on knebelite from Bluebell mine, British Columbia. *Can. Mineral.* **14**, 479-486.

NELSON, J., FERRI, F. & ROBACK, R. (1995): Late Paleozoic arc and oceanic terranes and their external relationships, southern Quesnellia. *Geol. Assoc. Can. – Mineral. Assoc. Can., Field Trip Guidebook* **B2**, 2-7.

NESBITT, B.E. & MUEHLENBACHS, K. (1989a): Origins and movement of fluids during deformation and metamorphism in the Canadian Cordillera. *Science* **245**, 733-736.

_____ & _____ (1989b): Geology, geochemistry, and genesis of mesothermal lode gold deposits of the Canadian Cordillera: evidence for ore formation from evolved meteoric water. *Econ. Geol., Monogr.* **6**, 553-563.

OHMOTO, H. & RYE, R.O. (1970): The Bluebell mine, British Columbia. I. Mineralogy, paragenesis, fluid inclusions, and the isotopes of hydrogen, oxygen, and carbon. *Econ. Geol.* **65**, 417-437.

ORR, K.E. & CHENEY, E.S. (1987): Kettle and Okanogan domes, northeastern Washington and southern British Columbia. *Washington Div. Geol. Earth Resources, Bull.* **77**, 55-71.

PARRISH, R.R., CARR, S.D. & PARKINSON, D.L. (1988): Eocene extensional tectonics and geochronology of the southern Omineca belt, British Columbia and Washington. *Tectonics* **7**(2), 181-212.

RASMUSSEN, M.G. (1993): *The Geology and Origin of the Overlook Gold Deposit, Ferry County, Washington.* Ph.D. dissertation, Univ. Washington, Seattle, Washington.

_____ (1995): Tertiary hydrothermal alteration and partial remobilization of Permian VMOS mineralization at the Overlook gold deposit, Ferry County, Washington. *In* Geology and Ore Deposits of the American Cordillera (Reno, Nevada). Geological Society of Nevada, U.S. Geological Survey, and Sociedad de Geologica de Chile, Abstracts and Symposium Volume.

ROBACK, R.C. & WALKER, N.W. (1995): Provenance, detrital zircon U–Pb geochronometry, and tectonic significance of Permian to lower Triassic sandstone in southeastern Quesnellia, British Columbia and Washington. *Geol. Soc. Am., Bull.* **107**, 665-675.

ROBIE, R.A., FINCH, C.B. & HEMINGWAY, B.S. (1982): Heat capacity and entropy of fayalite (Fe_2SiO_4) between 5.1 and 383 K: comparison of calorimetric and equilibrium values for the QFM buffer reaction. *Am. Mineral.* **67**, 463-469.

_____, HEMINGWAY, B.S. & FISHER, J.R. (1978): Thermodynamic properties of minerals and related substances at 298.15 K and 1 bar (10^5 pascals) pressure and at higher temperatures. *U.S. Geol. Surv., Bull.* **1452.**

RUSSELL, A. (1946): On rhodonite and tephroite from Treburland manganese mine, Altarnum, Cornwall; and on rhodonite from other localities in Cornwall and Devonshire. *Mineral. Mag.* **27**, 221-235.

SCOTT, S.D. (1973): Experimental calibration of the sphalerite geobarometer. *Econ. Geol.* **68**, 466-474.

SHANNON, F.G. (1970): Some unique geological features at the Bluebell mine, Riondel, British Columbia. *State of Washington Div. Mines, Bull.* **61**, 107-120.

SLACK, J.F., FLOHR, M.J.K. & SCULLY, M.V. (1997): Hypogene mineralogy and paragenesis of the Bald Mountain massive sulfide deposit, Aroostock County, Maine. *U.S. Geol. Surv., Open-File Rep.* **97-746.**

THIERRY, P., CHATILLON-COLINET, C., MATHIEU, J.C., REGNARD, J.R. & AMOSSÉ, J. (1981): Thermodynamic properties of the forsterite – fayalite ($Mg_2SiO_4 – Fe_2SiO_4$) solid solution. Determination of heat of formation. *Phys. Chem. Minerals* **7**, 43-46.

TOULMIN, P., III & BARTON, P.B., JR. (1964): A thermodynamic study of pyrite and pyrrhotite. *Geochim. Cosmochim. Acta* **28**, 641-671.

WHEELER, J.O., BROOKFIELD, A.J., GABRIELSE, H., MONGER, J.W.H., TIPPER, H.W. & WOODSWORTH, G.J., compilers (1991): Terrane map of the Canadian Cordillera. *Geol. Surv. Can., Map* **1713A** (scale 1;2,000,000).

WINGATE, M.T.D. & IRVING, E. (1994): Extension in high-grade terranes of the southern Omineca Belt, British Columbia: evidence from paleomagnetism. *Tectonics* **13**, 686-711.

YODER, H.S., JR. (1957): Isograd problems in metamorphosed iron-rich sediments. *Carnegie Inst. Wash., Year Book* **56**, 232-237.

Received July 29, 1997, revised manuscript accepted January 25, 1998.